Stable and high-order accurate finite difference schemes on singular grids

By M. Svärd AND E. van der Weide

1. Motivation and objectives

The use of finite difference methods on curvilinear grids is an established computational method and the technique has been thoroughly analyzed with respect to accuracy and stability. However, coordinate mappings are usually assumed to be smooth and topology conserving, such that a smooth mapping to a square grid exists. For practical applications it is not always possible to construct grids with these properties and singularities are sometimes present in the metric coefficients. Yet, it is desirable to have a robust computational method on such grids and obtain high-quality solutions.

In particular, we will study the grid shown in Figure 1, which we will refer to as the circle segment. The circle segment can be viewed as the mapping from a Cartesian grid where one side is collapsed into a point.

We will use a certain kind of finite difference schemes satisfying a summation-by-parts (SBP) rule. In combination with the Simultaneous Approximation Term technique (SAT), these schemes can be proven stable using energy estimates. The SAT technique use penalty terms to impose the boundary conditions weakly. (For SBP-SAT theory see Carpenter et al. 1994; Carpenter & Nordström 1999; Kreiss & Scherer 1974; Mattsson et al. 2006; Nordström & Carpenter 1999; Strand 1994; Svärd 2004; Svärd & Mattsson 2005; Svärd & Nordström 2006.) For such schemes, we will propose two different ways to recover design order accuracy despite singularities in the grid. The first is designed for SBP-SAT schemes and can be used at boundaries where boundary conditions are supplied. The other can be applied to any boundary and any stable finite difference scheme.

2. Summation-by-parts discretization

Before studying singular grid transformations, we introduce the basic concepts of SBP-SAT schemes. Discretize $0 \leq x \leq 1$ using $N+1$ evenly distributed grid points with spacing h. Introduce the scalar grid function $v(t) = (v_0(t), ..., v_N(t))^T$. Then the first derivative is approximated by, $P^{-1}Qv$, where P is a positive definite (symmetric) matrix. P is used to define a discrete l_2 equivalent norm, $\|v\|_P^2 = v^T P v$. In our particular schemes P is diagonal, which is a necessary requirement for stability on curvilinear grids. (See Svärd 2004.) Q is skew-symmetric almost everywhere and $Q + Q^T = diag(-1, 0, ..., 0, 1) = B$. In two space dimensions, we use a subscript x or y to distinguish between operators in the respective directions.

As a model problem for the non-linear two-dimensional Euler equations, we consider,

$$u_t + a(x,y)u_x + b(x,y)u_y = 0, \;\; 0 \leq x, y, \leq 1, \;\; t \geq 0, \tag{2.1}$$

where $a(x,y), b(x,y) > 0$. The equation is subject to the following boundary conditions,

$$u(0,y,t) = g_1(y,t), \quad u(x,0,t) = g_2(x,t).$$

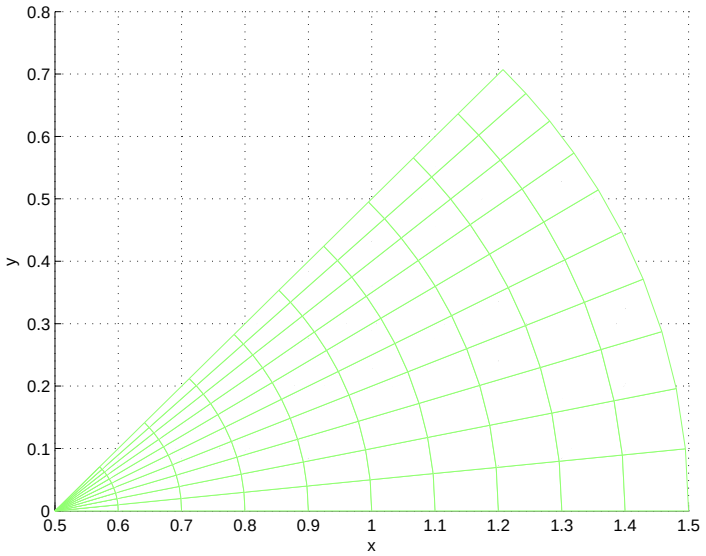

FIGURE 1. A grid with a collapsed side.

We discretize the equation using N points in the x-direction and M in the y-direction. We denote the grid sizes by $h_x = 1/N$ and $h_y = 1/M$. Let $v_{ij}(t)$ be the approximate solution of $u(x_i, y_j, t)$ and v be the vector $v = (v_{00}, v_{20}, ..., v_{NM})$. Define $a_{ij} = a(x_i, y_j)$ and $b_{ij} = b(x_i, y_i)$ and distribute a_{ij} and b_{ij} on the diagonal of a matrix in the same way v_{ij} was distributed. Denote the resulting matrices A and B. The discretization of (2.1) can be written.

$$\begin{aligned} v_t + A(I \otimes D_x)v + B(D_y \otimes I)v = \\ \tau_1(I \otimes P^{-1}E_{0x})(v - G_1) + \tau_2(P^{-1}E_{0y} \otimes I)(v - G_2) \end{aligned} \tag{2.2}$$

where $E_{0y}v = (v_{0,0}, .., v_{N,0})^T$. $E_{0x} = (v_{0,0}, 0, ..., v_{0,1}, 0, ..., v_{0,M}, 0...)^T$. The symbol $\otimes$ denotes the Kronecker product. Moreover, G_1 and G_2 are vectors with $(G_1)_{0j} = g_1(y_j, t)$ and $(G_2)_{i0} = g_2(x_i, t)$ and 0 elsewhere.

To prove stability, we freeze the coefficents in A and B (and denote the respective scalars by a and b) and apply the energy method by multiplying by $v^T(P_y \otimes P_x)$,

$$\begin{aligned} (\|v\|^2_{P_{xy}})_t + av^T(P_y \otimes B_x)v + bv^T(B_y \otimes P_x) = \\ 2\tau_1(P_y \otimes E_{0x})(v - G_1) + 2\tau_2(E_{0y} \otimes P_x)(v - G_2) \end{aligned} \tag{2.3}$$

In (2.3) we have introduce the norm $\|v\|^2_{P_{xy}} = v^T(P_y \otimes P_x)v$. Assuming homogeneous data, $\tau_1 \leq -a/2$ and $\tau_2 \leq b/2$ guarantees stability.

In this article, we will use two different schemes. The first is the commonly used central second-order stencil with a first order boundary closure. We will refer to this schemes as the 2-1 method. The other is the standard central difference fourth-order accurate scheme with a specific second-order boundary closure that enforces the SBP property. This scheme is called the 4-2 method. In both cases the norm P is diagonal and the precise form of operators (P and Q) can be found in Strand (1994).

2.1. *Grid singularities*

Consider,

$$u_t + au_x + bu_y = 0. \tag{2.4}$$

Assume $0 \leq a \leq 1$ and $b = -\sqrt{1-a^2}$. The exact solution is, $u(x,t) = sin(ax + by - t)$. Introduce $x = x(\xi,\eta)$, $y = y(\xi,\eta)$. Then (2.4) can be written as,

$$u_t + a(\xi_x u_\xi + \eta_x u_\eta) + b(\xi_y u_\xi + \eta_y u_\eta) = 0 \tag{2.5}$$

We define $J = (x_\xi y_\eta - x_\eta y_\xi)$ and obtain,

$$J\xi_x = y_\eta,\ J\xi_y = -x_\eta,\ J\eta_x = -y_\xi,\ J\eta_y = x_\xi, J = (\xi_x\eta_y - \xi_y\eta_x)^{-1}.$$

In the circle segment (Figure 1) we have ξ and η being the polar coordinates r and θ with the transformation $(x,y) = (rcos(\theta) + 0.5, rsin(\theta))$, $r = [0,1], \theta = [0,\pi/4]$. In this case, $\frac{\partial r}{\partial x} \sim 1$, $\frac{\partial r}{\partial y} \sim 1$, $\frac{\partial \theta}{\partial x} \sim \frac{1}{r}$, $\frac{\partial \theta}{\partial y} \sim \frac{1}{r}$. We rewrite equation (2.5),

$$u_t + \hat{a}u_\xi + \hat{b}u_\eta = 0, \quad \hat{a} = a\xi_x + b\xi_y, \quad \hat{b} = a\eta_x + b\eta_y. \tag{2.6}$$

Equation (2.6) is now a variable coefficient problem in ξ,η-space and we wish to employ the same discretization technique as for (2.1). However, $\hat{a}$ and $\hat{b}$ may now be singular.

We will study the effect of the following approximation. *At the singular point, approximate the indefinite metric coefficents with the coefficients of non-singular neighbors.* This is a first-order approximation of the metrics and the truncation error of the approximation of the equation reduces to first order at that point.

For the circle segment (Figure 1), we note that the transformation from the square makes $x = 0.5, y = 0$ a multi-valued point, since all the points on that side collapse to one. Let $(x(i,j), y(i,j))$, $i = 0...N, j = 0..M$ be a grid point. Then $(x(0,j), y(0,j)) = (x(0,k), y(0,k))$ for any valid combination j,k. With that notation, we choose,

$$y_\eta(x(0,j), y(0,j)) = y_\eta(x(1,j), y(1,j)), \quad x_\eta(x(0,j), y(0,j)) = x_\eta(x(1,j), y(1,j)).$$

3. Analysis

To study the basic mechanisms of singular coordinate transformations, we consider the one-dimensional problem,

$$u_t + u_x = 0, \quad t \geq 0,\ 0 \leq x \leq \infty. \tag{3.1}$$

Introduce a coordinate transformation $x = x(\xi)$ such that,

$$u_t + \xi_x u_\xi = 0, \quad t \geq 0,\ \xi_1 \leq \xi \leq \xi_2. \tag{3.2}$$

Let $x = \xi^2/2$ such that $x_\xi = \xi$. Furthermore, $\xi_x = x_\xi^{-1} = \frac{1}{\xi}$. This motivates the study of the following problem,

$$u_t + \frac{1}{x}u_x = 0, \quad t \geq 0,\ 0 \leq x \leq \infty. \tag{3.3}$$

In this case the coefficient in front of u_x becomes singular as $x \to 0$. However, in the circle segment case it is the coefficent in front of the u_η that becomes singular as $r \to 0$. This fact suggests that also the following model problem is relevant to analyze.

$$u_t + \frac{1}{y}u_x = 0, \quad t \geq 0,\ 0 \leq x, y \leq \infty. \tag{3.4}$$

We will also study,

$$u_t + au_x = 0, \quad t \geq 0,\ 0 \leq x \leq \infty,\ a > 0, \tag{3.5}$$

which will give us insight in the properties of the penalty imposition of boundary conditions. Equation (3.5) will be referred to as Model Problem 1, since it is the simplest to analyze. Morevoer, (3.3) is denoted Model Problem 2 and (3.4) Model Problem 3.

3.1. *Model problem 1*

Consider (3.5) and assume that $u \to 0$ sufficiently fast as $x \to \infty$. We use the exact solution $u(x,t) = sin(ax - t)$ to provide initial and boundary data. We discretize using the SBP-SAT methodology.

$$v_t + aP^{-1}Qv = \tau P^{-1}E_0(v - g) \tag{3.6}$$

where $E_0 = diag(1, 0, ..., 0)$. Assuming homogeneous data, the energy estimate becomes,

$$(\|v\|_P^2)_t - av_0^2 + av_0^2 = 2\tau v_0^2. \tag{3.7}$$

For $\tau \leq -a/2$ the scheme is stable. The 2-1 scheme can be proven to have a globally second-order convergence rate and the 4-2 third order. (See Gustafsson 1975, 1981; Svärd & Nordström 2006.) We define the convergence rate, $q = |log(e_1/e_2)/log(h_1/h_2)|$ where e_1 and e_2 are the errors (in an appropriate norm) on two different grids with grid sizes h_1 and h_2. The numerical solution using the two different schemes are computed using the standard fourth-order explicit Runge-Kutta scheme in time, with a time step small enough for the temporal errors to be negligible. (Correct convergence rates have been shown for these schemes.) Our proposed remedy, for the coordinate singularity was to make a first-order approximation of the metric coefficents, i.e. to lower the accuracy of the approximation of the partial differential equations at that point. To model that, we add an order 1 error (a constant c) to the equations at the boundary point. The stability properties are not changed by the addition of a lower order term. According to classical theory Gustafsson (1975, 1981), the resulting order of accuracy should be 1. We will now analyze this case in detail. Let u be the exact solution and define the error $e_k(t) = u(x_k, t) - v_k(t)$ and the vector $e = (e_1, e_2, ...)^T$. Then the error equation is,

$$e_t + aP^{-1}Qe = \tau P^{-1}E_0(e - 0) + T,$$

where T is the truncation-error vector with the constant c at the boundary point included. Hence, $T = (\mathcal{O}(1), \mathcal{O}(h^2), ...)^T$. Next, we split the truncation error into two parts, $T = T_i + T_b$, where, $T_i = (\mathcal{O}(1), 0, ...)^T$, $T_b = (0, \mathcal{O}(h^2), ...)^T$. Correspondingly, we let $e = e_i + e_b$ and split the problem into,

$$(e_i)_t + aP^{-1}Qe_i = \tau P^{-1}E_0(e_i - 0) + T_i, \tag{3.8}$$
$$(e_b)_t + aP^{-1}Qe_b = \tau P^{-1}E_0(e_b - 0) + T_b, \tag{3.9}$$

Note that, e_i and e_b are in general non-zero everywhere since there is usually a strong coupling between the interior and the boundary. It follows directly from the energy estimate of (3.8) that e_i is of order T_i, i.e. second-order in this case. Let $(P^{-1})_{00} = (hp)^{-1}$ where p is a constant. ($p = 1/2$ for the 2-1 scheme and $p = 17/48$ for the 4-2 scheme.)

N	$\tau = -a$ l_2-error	q_2	l_∞-error	q_∞	$\tau = -a/h$ l_2-error	q_2	l_∞-error	q_∞
10	0.0025	-	0.0071	-	9.8062e-04	-	0.0029	-
20	0.0010	1.3219	0.0035	1.0205	2.2634e-04	2.1152	7.7750e-04	1.8991
40	4.2519e-04	1.2338	0.0016	1.1293	5.1196e-05	2.1444	1.8462e-04	2.0743
80	2.0653e-04	1.0418	7.7984e-04	1.0368	1.2834e-05	1.9961	4.7078e-05	1.9714
160	1.0075e-04	1.0356	3.9445e-04	0.9833	3.1810e-06	2.0124	1.2239e-05	1.9436
320	4.9906e-05	1.0135	1.9911e-04	0.9863	7.9385e-07	2.0025	3.0348e-06	2.0118

TABLE 1. Errors and convergence rates at $t = 0.1$ for the 2-1 discretization of the advection equation with $a = 1$ and zeroth-order boundary error.

For e_b we proceed by Laplace transforming (3.9).

$$s(\hat{e}_b)_i + a\frac{(\hat{e}_b)_{i+1} - (\hat{e}_b)_{i-1}}{2h} = (\hat{T}_b)_i = 0,\ i \geq 1 \tag{3.10}$$

$$s(\hat{e}_b)_0 + a\frac{(\hat{e}_b)_1 - (\hat{e}_b)_0}{h} = \tau\frac{(\hat{e}_b)_0}{ph} + (\hat{T}_b)_0, \tag{3.11}$$

We make the following ansatz, $(\hat{e}_b)_i = \sigma\kappa^i$ and define $\tilde{s} = sh/a$. At the left boundary all κ with $|\kappa| < 1$ for $Re\,\tilde{s} > 0$ should be supplied with boundary conditions. If σ is bounded for $Re\,\tilde{s} \geq 0$ the scheme is stable. (See Gustafsson et al. 1995.) We use the ansatz in (3.10) and obtain $\kappa = -\frac{\tilde{s}}{a} \pm \sqrt{\frac{\tilde{s}^2}{a^2} + 1}$ It can be shown that $\kappa_1 = -\frac{\tilde{s}}{a} + \sqrt{\frac{\tilde{s}^2}{a^2} + 1} < 1$, for $Re\,\tilde{s} > 0$. We use the definition that the square root denotes the value with positive real part. (In this case $\sigma_2 = 0$ corresponding to κ_2 due to the fall-off condition of u. Otherwise, it is bounded by the right boundary condition.) We insert $(\hat{e}_b)_i = \sigma_1\kappa_1^i$ in (3.11), and use the expression for κ_1,

$$\sigma_1(\sqrt{\frac{\tilde{s}^2}{a^2} + 1} - 1 - \frac{\tau}{ap}) = \frac{h(T_b)_0}{a}.$$

Denote the resolvent $R = (\sqrt{\frac{\tilde{s}^2}{a^2} + 1} - 1 - \frac{\tau}{ap})$. For $Re\,\tilde{s} \geq 0$ we have that $Re\sqrt{\frac{\tilde{s}^2}{a^2} + 1} \geq 0$. Hence, $\sigma_1 \neq 0$ if $-1 - \frac{\tau}{ap} > 0$, i.e $\tau < -a/2$. This is in full agreement with the stability analysis using the energy estimate. Choosing $\tau = constant < -a/2$ implies that R is of order 1 and $\sigma_1 \sim \frac{h(T_b)_0}{a}$. If $(T_b)_0$ is of order h we have $\sigma_1 \sim h^2$. Hence, $\hat{e}_b \sim h^2$. Transforming back using Parseval's relation, we obtain that e_b is second-order accurate. This is the classical result that a scheme is allowed to be closed with 1 order less accuracy at the boundary without degrading the global accuracy. (See Gustafsson 1975, 1981 and also Svärd & Nordström 2006.)

In our example, $(T_b)_0 \sim 1$ implying that $\hat{e}_b$ and consequently e_b is $\mathcal{O}(h)$. In Table 2 this case is computed, corrobating the expected first-order convergence rate. We use $c = 0.1$ as the order 1 error, $a = 1$, $\tau = -a$.

Next, we consider the case $\tau = -a/(h^p) < -a$. Now, $R \sim 1/(h^p)$ and $\sigma \sim h^{p+1}(T_b)_0$. In our case with zeroth-order boundary closure and $p = 1$ we recover second-order global accuracy, see Table 1. Of course, there is little to gain by choosing a larger p since the global order of accuracy is also limited by the interior accuracy. To show that these conclusions carry over to high-order finite difference methods, we compute a similar

τ	$-a$	$-a$	$-a/h$	$-a/h$
N	l_2-error	q_2	l_2-error	q_2
10	1.0220e-04	-	5.1669e-05	-
20	2.7002e-05	1.9203	9.0017e-06	2.5210
40	7.0084e-06	1.9459	1.3840e-06	2.7014
80	1.7607e-06	1.9929	1.7674e-07	2.9691
160	4.3989e-07	2.0009	2.2384e-08	2.9811
320	1.0973e-07	2.0032	2.8176e-09	2.9899

TABLE 2. Errors and convergence rates at $t = 0.1$ for the 4-2 discretization of the advection equation with $a = 1$ and first-order boundary error. Different scalings of the penalty parameter, τ.

example using the 4-2 scheme. For the 4-2 scheme, we add, $0.1h$ to the first point in the scheme, i.e. a first-order error, and compute the solution with different scalings of the penalty term, see Table 2. As expected the convergence rate drops to 2 with $\tau = -a$. Third-order convergence it recovered for $\tau = -a/h$.

3.2. *Model problem 2*

The previous example shows a fundamental phenomenon that order of accuracy may be increased via a stronger enforcement of the penalty boundary conditions. However, we assumed that $a(x) = a$ and we may only claim that the analysis holds for a case where $a(x)$ is smooth. But, in the coordinate transformation case the $a(x)$ becomes singular. Hence, we continue our analysis and consider Model Problem 2 (3.3) and observe that $u(x,t) = sin(\frac{x^2}{2} - t)$ is the solution. Obviously, (3.3) is singular at $x = 0$. Let $x_i = ih$ and $a(x_i) = 1/x_i$ for $i = 1, ..., N$ and $a(x_0) = 1/x_1$, which is a first-order approximation. Define $A = diag(a(x_0), a(x_1), ..., a(x_N))$. We discretize (3.3) as,

$$v_t + AP^{-1}Qv = \tau P^{-1}E_0(v - g) \tag{3.12}$$

Since A^{-1} and P are diagonal and positive definite, we can define a norm $\|v\|^2 = v^T A^{-1} P v$. Then we use the energy method with homogenoues data and arrive at,

$$\|v\|_t^2 - v_0^2 + v_N^2 = 2\tau a^{-1}(x_0)v_0^2 \tag{3.13}$$

The scheme is stable if $\tau \leq -1/(2a^{-1}(x_0))$. Since $a^{-1}(x_0) = x_1 = h$ we have, $\tau \leq -1/(2h)$. This stability limit is easily verified in computations and is valid for both the 2-1 method and 4-2 method. In the 2-1 case the first-order closure of A is sufficient for globally second-order convergence. However, in the 4-2 case the convergence drops from third to second order, see Table 3. Note also that the stablity limit of τ is dependent on the strength of the singularity. In this case $a(x) = 1/x$ implies that $\tau \sim 1/h$. But, if $a(x) = 1/\sqrt{x}$ we would obtain $\tau \sim 1/\sqrt{h}$, and so on.

Next, we consider the possiblity to raise the order of accuracy at the boundary by increasing the strength of τ as a function of h. Again, we consider the boundary portion of the error equation for the quarter-space problem. (The interior can readily be shown to give the correct convergence rate via the energy estimate.)

$$(e_i)_t + \frac{1}{x_i}\frac{e_{i+1} - e_{i-1}}{2h} = 0,\ i > 1,\ \ (e_0)_t + \frac{1}{x_1}\frac{e_1 - e_0}{h} = \frac{\tau}{ph}e_0 + T_0,\ i = 0, \tag{3.14}$$

τ	$-1/h$	$-1/h$	$-1/h^2$	$-1/h^2$
N	l_2-error	q	l_2-error	q
10	0.0025	-	2.7040e-04	-
20	6.1073e-04	2.0333	3.9040e-05	2.7921
40	1.4964e-04	2.0290	4.7133e-06	3.0501
80	3.7125e-05	2.0110	6.2343e-07	2.9184

TABLE 3. Errors and convergence rates at $t = 0.1$ for the 4-2 scheme with $a = 1/x$ and first-order approximation of metrics at $x = 0$.

Laplace transform the first equation in (3.14) results in $\kappa(i) = -\tilde{s}x_i \pm \sqrt{(\tilde{s}x_i)^2 + 1}$. Again, $|\kappa_1| = |-\tilde{s}x_i + \sqrt{(\tilde{s}x_i)^2 + 1}| < 1$ and $Re\,\sqrt{(\tilde{s}x_i)^2 + 1} > 0$, since $x_i > 0$. We note that according to our approximation $x_0 = x_1 = h$. Laplace transforming equation (3.14) and using the explicit expression for κ_1 yield,

$$\sigma(\frac{\sqrt{(\tilde{s}h)^2 + 1} - 1}{h} - \frac{\tau}{p}) = h\hat{T}_0,\ i = 0,\ t \geq 0$$

For stability, we demand that the resolvent, $R = (\frac{\sqrt{(\tilde{s}h)^2+1}-1}{h} - \frac{\tau}{p}) > 0$, for $Re\,\tilde{s} \geq 0$, $h \geq 0$. Since $Re\,\sqrt{(\tilde{s}h)^2 + 1} \geq 0$ we must require that, $-\frac{1}{h} - \frac{\tau}{p} > 0$ and obtain $\tau < -p/h = -1/(2h)$. With $\tau \sim 1/h$ we have $R \sim 1$ and $\sigma \sim hT_0$. Using Parseval's relation, we also obtain that $e_b \sim h\hat{T}_0$.

As in the constant coefficent case we may choose $\tau \sim 1/h^p$ to obtain $e_b \sim h^{p+1}T_0$. With $\tau = -1$ the scheme is unstable as predicted by theory and the results $\tau = -1/h$ and $\tau = -1/h^2$ are displayed in Table 3. The results supports the theoretical derivations.

3.3. *Model problem 3*

The polar singularity was modelled by, $u_t + \frac{1}{y}u_x = 0$, $0 \leq x, y \leq 1$. This equation is discretized as outlined in (2.2). We choose $A = diag(a(y_0), ..., a(y_M))$, where $a(y_0) = 1/y_1$ and $a(y_i) = 1/y_i$, $i = 1..M$. That is, we commit a first-order error along the line $y = 0$. We need boundary conditions at $x = 0$ and choose $\tau_1 = -a(y_i)$ at y_i in (2.2). Further, $\tau_2 = 0$ in (2.2). We use the exact solution $u = sin(yx - t)$ to provide boundary and intitial data. We do not need to redo a similar analysis but only interpet this case from the results of the constant coefficient. For each $y \neq 0$ the equation is approximated to design order. If we assume that the 4-2 is employed, we have third-order global convergence. In other words, for $N \times M - 1$ points the error is $\mathcal{O}(h_x^3)$. For $y = 0$ we approximate $1/y$ by $1/y_1 = 1/h_y$ and we commit a first-order error on N points. We assume that $h_x \sim h_y \sim h$. Then the overall l_2-error, e_{l_2}, is computed as,

$$e_{l_2}^2 = h^2 \sum_{i=1}^{N} \sum_{j=1}^{M} e_{ij}^2 \sim h^2 \left(N(M-1)(h^3)^2 + N(h)^2 \right) \sim h^2(h^4 + h) \sim h^3$$

or, $e_{l_2} \sim h^{1.5}$. The computational results are displayed in Table 4 and the convergence rate is 1.5 as predicted. As mentioned above, we need not supply any boundary condition at $y = 0$. However, at any boundary we may enforce the exact solution, if known, as a

N	error	q
10	0.0195	-
20	0.0067	1.5412
40	0.0023	1.5425
80	8.1073e-04	1.5043

TABLE 4. Errors and convergence rates at $t = 0.1$ for the 4-2 scheme with $a = 1/y$ and first-order approximation of $1/y$ at $y = 0$.

N	error	q
10	0.0011	-
20	1.9677e-04	2.4829
40	3.4801e-05	2.4993
80	6.1540e-06	2.4995

TABLE 5. Errors and convergence rates at $t = 0.1$ for the 4-2 method with $a = 1/y$ and first-order approximation of $1/y$ at $y = 0$. A penalty term enforce the exact solution along the slip boundary $y = 0$.

boundary condition. In this case we know the exact solution and we choose $\tau_2 = -a(y_0)$. As the previous analysis suggests, we should gain one order of accuracy at $y = 0$ (and globally.) We note that Table 5 supports that conclusion.

3.4. *Advection equation on the circle segment*

We will compute the solution to the advection equation with the 4-2 method on the circle segment shown in Figure 1. The grid spacing is equidistant meaning $\Delta r = constant$ and $\Delta\phi = constant$ with $N + 1$ points in both directions, implying that $h_\xi = h_\eta = 1/N$. (The general coordinate ξ corresponds to r and η to θ.) We use the scheme (2.2) for the equation (2.6) with $a = 0.9$ and $b = -\sqrt{1 - a^2}$ and compute two different cases:

(*a*) $(\tau_1)_j = -\hat{a}(x_0, x_j)$ and $(\tau_2)_i = \hat{b}(x_i, y_N)$. (A local penalty parameter is computed at each gridpoint.)

(*b*) $(\tau_1)_j = -\hat{a}(x_0, x_j)/h_\xi$ and $(\tau_2)_i = \hat{b}(x_i, y_N)$.

In the first case, we commit an $\mathcal{O}(h)$ error along the line $\xi = 0$. The penalty strength at $\xi = 0$ is the marginal scaling for stability. Hence, this case corresponds to Model Problem 3 without the extra penalty term at $y = 0$. We would expect the l_2 convergence rate to be 1.5 and the l_∞ convergence rate to be 1, which is the case in Table 6.

The second case corresponds to Model Problem 3 with the additional penalty at $y = 0$ in the sense that the penalty is unecessary strong for pure stability purposes. However, the effect is an increased convergence rate by one order in both l_2 and l_∞, which is observed in Table 7.

3.5. *Grid singularity at outflow boundary.*

So far, we have only considered the case of a grid with boundary condition at the singularity. To study the case of a grid singularity at an outflow we consider Model Problem

N	l_2-error	q_2	l_∞-error	q_∞
10	0.0068	-	0.0292	-
20	0.0024	1.5025	0.0142	1.0401
40	8.5049e-04	1.4967	0.0071	1.000
80	3.0001e-04	1.5033	0.0036	0.9798

TABLE 6. Errors and convergence rates on the circle segment grid at $t = 0.1$ for the 4-2 method with $(\tau_1)_j = -\hat{a}(x_0, x_j)$.

N	l_2-error	q_2	l_∞-error	q_∞
10	0.0012	-	0.0057	-
20	2.2791e-04	2.3965	0.0016	1.8329
40	4.2458e-05	2.4244	4.5839e-04	1.8034
80	7.7408e-06	2.4555	1.2366e-04	1.8902

TABLE 7. Errors and convergence rates on the circle segment grid at $t = 0.1$ for the 4-2 method with $(\tau_1)_j = -\hat{a}(x_0, x_j)/h_\xi$.

2, modified to a left-going wave problem.

$$u_t - a(x)u_x = 0, \quad a(x) = \frac{1}{x}, \quad u(1,t) = g(t), \quad 0 \le x \le 1 \tag{3.15}$$

The idea is to try to increase the accuracy of the approximated metric coefficient at the left boundary. The naive approach is to extrapolate to higher order using the ansatz, $a(x_0) \approx \alpha a(x_1) + \beta a(x_2)$, and Taylor expand.

$$\begin{aligned} a(x_0) \approx \alpha(a(x_0) + a'(x_0)(x_1 - x_0) + a''(x_0)\frac{(x_1 - x_0)^2}{2}) \\ +\beta(a(x_0) + a'(x_0)(x_2 - x_0) + a''(x_0)\frac{(x_2 - x_0)^2}{2}). \end{aligned} \tag{3.16}$$

We have to interpret the derivatives as limits as $x_0 \to 0$. Then we obtain the conditions,

$$\alpha + \beta = 1, \quad \alpha h + 2h\beta = 0, \quad \alpha = 2, \beta = -1. \tag{3.17}$$

This is the same solution we would obtain if we had fit a linear polynomial between x_1 and x_2 and extrapolated to x_0. The Taylor expansions, however, gives insight in the errors commited. The convergence rates obtained using this kind of extrapolation is shown in Table 8. p is the order of the extrapolation polynomial, i.e. $p = 0$ is the previously used simple extrapolation from a close neighbor. $p = 1$ the linear extrapolation derived above, and $p = 2$ a second-order polynomial. As is clearly seen, trying to extrapolate to higher order does not raise the accuracy. To explain these results, we consider the first error term of (3.16).

$$e = \alpha a''(x_0)\frac{(x_1 - x_0)^2}{2} + \beta a''(x_0)\frac{(x_2 - x_0)^2}{2}. \tag{3.18}$$

Let x_0 approach 0 and compute the limit, $e = \alpha\frac{1}{h} + \beta\frac{1}{2h}$. We conclude that the error at x_0 is a term $a(x_0 + h)$, i.e. a first order error, which explains the results in Table 8. Of

p	0	0	1	1	2	2
N	l_2-error	q	l_2-error	q	l_2-error	q
11	0.0024	-	0.0016	-	0.0013	-
21	5.6173e-04	2.0951	3.7609e-04	2.0889	3.0830e-04	2.0761
41	1.3472e-04	2.0599	8.9812e-05	2.0661	7.3485e-05	2.0688
81	3.3056e-05	2.0270	2.2041e-05	2.0267	1.8035e-05	2.0267

TABLE 8. Eq (3.15) approximated with the 4-2 scheme. Extrapolation of $-1/x$ to $x = 0$ with polynomial order p.

N	l_2-error	q_2
11	2.9288e-04	-
21	3.5629e-05	3.0392
41	3.7477e-06	3.2490
81	4.4241e-07	3.0825

TABLE 9. Eq (3.15) approximated with the 4-2 scheme. $-1/h^2$ approximating $-1/x$ at $x = 0$.

$\sqrt{N}$	l_2-error	q_2	l_∞-error	q_∞
11	0.0024	-	0.0136	-
21	8.3055e-04	1.5309	0.0068	1.000
41	2.8687e-04	1.5337	0.0034	1.000
81	1.0012e-04	1.5187	0.0017	1.000
161	3.5161e-05	1.5097	8.4251e-04	1.0128

TABLE 10. Circle segment with outflow at singular point ($a = -1, b = 0$). Zeroth-order interpolation of y_η, x_η to $x = 0.5, y = 0$.

course, extrapolation only gives smaller leading error term with higher polynomial order if the extrapolated function is sufficiently smooth, which was not the case above. This leads us to extrapolate the smooth inverse of $1/x$.

That is, we approximate $x_0 = 0$ to second order accuracy, i.e. $x_0 \equiv x' = h^2$, such that $1/x_0$ is approximated by $1/x' = 1/h^2$ which is a second-order approximation and the entire scheme should recover third-order accuracy. Indeed, this is confirmed in Table 9. Again, the numerical scheme becomes more stiff. Applying the same idea to the circle segment suggest that y_η and x_η should be extrapolated to second-order accuracy. In our example the functions are linear and we use a linear extrapolation to a point $\mathcal{O}(\Delta r^2)$ away from the singularity. The results are displayed in Table 10 and 11. As is seen we get the predicted convergence rate 2 in l_∞. We have confirmed that the maximum errors occur at the singular point and get an approximate convergence rate of 2.5 in l_2.

$\sqrt{N}$	l_2-error	q_2	l_∞-error	q_∞
11	3.8502e-04	-	0.0022	-
21	7.2143e-05	2.4160	5.8375e-04	1.9141
41	1.3120e-05	2.4591	1.4845e-04	1.9754
81	2.7956e-06	2.2305	3.7411e-5	1.9884

TABLE 11. Circle segment with outflow at singular point ($a = -1, b = 0$). Linear interpolation of y_η, x_η to a point h^2 away from $x = 0.5, y = 0$.

3.6. *Time step limits*

Both the proposed remedies for the grid singularity introduces a stiffnes to the problem, if compared to the same problem on a non-singular grid. However, if we accept the choice of a singular grid transformation and still want to compute a solution, the time step restriction is unavoidable. Consider,

$$u_t + a(x)u_x = 0 \tag{3.19}$$

Then the CFL constraint is $\Delta t < c \cdot a(x)/h$ where c is a constant depending on the choice of numerical scheme. As an example, we use model problem 1 where $a(x) = 1/x$. The more accurate we want to approximate $a(0)$, the more stiff the problem becomes.

4. The Euler equations

We will demonstrate the robustness of the proposed techniques using the Euler equations of gas dynamics. We will consider an analytical vortex solution that enables us to measure the error. Since the flows will be subsonic there will be boundary conditions both at inflows and at outflows but not on all variables. Hence, we will use the technique where the metric coefficients are approximated (and not the remedy utilizing stronger penalties). The computations will be carried out with the multi-block SBP-SAT finite difference code SUmb. The Euler equations are stated on conservative form and since the previous analysis was carried out on primitive form, we will briefly discuss the differences with respect to the metric approximations. The Euler equations in a Cartesian system can be stated as,

$$u_t + F_x + G_y = 0 \tag{4.1}$$

where u are the conservative variables and F, G are the fluxes. Applying a coordinate transformation results in,

$$(Ju)_t + (J\xi_x F + J\xi_y G)_\xi + (J\eta_x F + J\eta_y G)_\eta = 0. \tag{4.2}$$

We note that $J\xi_x = y_\eta, J\xi_y = -x_\eta, J\eta_x = -y_\xi, J\eta_y = x_\xi$ are not singular but well-defined on the grids we have considered. Hence, it is only J appearing in the time derivative that is troublesome. To compute J, we use the approximations of the metric coefficients discussed at length above. We use the analytical solution as initial and boundary data. The Mach number is 0.5 and the solution is computed with the 4-2 scheme marched with a 3rd-order explicit Runge-Kutta scheme on 4 different meshes. The domain is seen in Figure 2 and the grid sizes are: 33×17 points (grid 1); 65×33 points (grid2); 129×65 points (grid 3); 257 × 129 points (grid 4). At $T = 0.6$ the l_2-errors, l_∞-errors and convergence

grid	l_∞-error	q	l_2-error	q
1	0.7263e-02	-	5.424e-4	-
2	0.2251e-02	1.69	2.032e-4	1.42
3	0.9573e-03	1.23	6.027e-5	1.75
4	0.4275e-03	1.16	1.921e-5	1.65

TABLE 12. l_2-errors, l_∞-errors and convergence rates for the Euler equations computed with the 4-2 schemes.

rates are displayed in Table 12. We note that the computational convergence rates, are close to the theoretical 1.5 in l_2 and 1 in l_∞. Also, the computations are perfectly stable on all grids and we note that the 4-2 method is quite accurate although the formal order is degraded due to the singularity. In Figure 2 the density is shown at $T = 0.6$ for two different grids: the coarsest (grid 1) and the second finest (grid 2). We observe that on grid 3 an almost perfect solution is obtained but even the solution on the coarsest mesh is good.

5. Conclusions

We have considered fictious singularities introduced by the mapping of a non-square computational grid to a square that results in singular metric coefficients. We approach this problem by studying one-dimensional model problems and present two ways of handling the singularity, while keeping design order of the scheme.

The first remedy is applicable to SBP-SAT schemes and requires only a crude and simple approximation of the metric coefficients (one can even choose them to be an arbitrary constant). The accuracy is recovered through a stronger enforcement of the penalty boundary conditions.

The second technique, is a sufficiently accurate extrapolation of the metric coefficients to a point that approaches the singularity sufficiently fast. This solution is generally applicable to any stable finite difference scheme. However, care has to be taken when the metric coefficents are extrapolated and naive extrapolations do not improve the accuracy. Numerical examples supports the linear analysis for both remedies.

Both methods yield a more stiff set of ordinary differential equations to solve, compared to the same problem on a non-singular grid. The additional stiffness is proportional to the strength of the singularity. We show that this is a natural CFL constraint.

Finally, we show how to interpret the results for a system of equations in conservative form. We demonstrate that the non-linear two-dimensional Euler equations computed with the 4-2 scheme is robust with the second technique and obey the same accuracy properties as the linear counterpart.

REFERENCES

Carpenter,M. H., Gottlieb, D. and Abarbanel, S. Time-stable boundary conditions for finite-difference schemes solving hyperbolic systems: Methodology and application to high-order compact schemes. *J. Comput. Phys.*, 111(2), 1994.

Carpenter, M.-H., Nordström, J. and Gottlieb, D. A Stable and Conservative Interface Treatment of Arbitrary Spatial Accuracy. *J. Comput. Phys.*, 148, 1999.

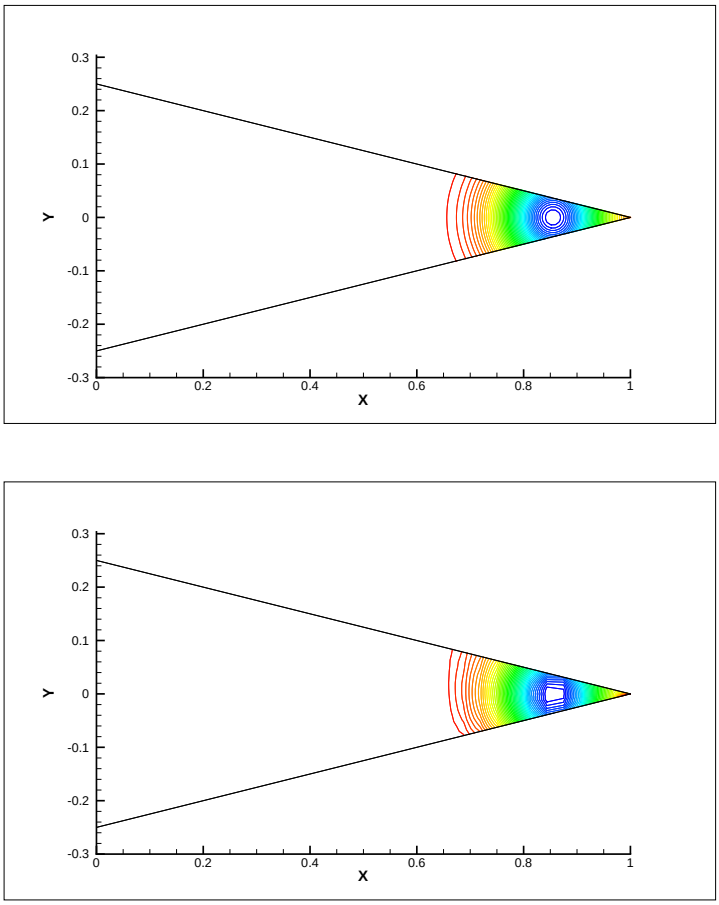

FIGURE 2. The density of the Euler vortex solution at $T = 0.6$. The top figure computed with the 4-2 method on Grid 3 and the bottom figure on Grid 1.

Gustafsson, B. The convergence rate for difference approximations to mixed initial boundary value problems. *Math. Comp.*, 29(130):396–406, Apr. 1975.

Gustafsson, B. The convergence rate for difference approximations to general mixed initial boundary value problems. *SIAM J. Numer. Anal.*, 18(2):179–190, Apr. 1981.

Gustafsson, B., Kreiss, H.-O. and Oliger, J. *Time dependent problems and difference methods*. John Wiley & Sons, Inc., 1995.

Kreiss, H.-O. and Scherer, G. Finite element and finite difference methods for hyperbolic partial differential equations. *Mathematical Aspects of Finite Elements in Partial Differential Equations., Academic Press, Inc.*, 1974.

Mattsson, K., Svärd, M., Carpenter, M. H. and Nordström, J. High-order accurate computations for unsteady aerodynamics. *in press Computers and Fluids*, 2006.

Nordström, J. and Carpenter, M. H. Boundary and interface conditions for high-order finite-difference methods applied to the Euler and Navier-Stokes equations. *J. Comput. Phys.*, 148, 1999.

Strand, B.. Summation by Parts for Finite Difference Approximations for d/d x. *J. Comput. Phys.*, 110, 1994.

Svärd, M. On coordinate transformation for summation-by-parts operators. *Journal of Scientific Computing*, 20(1), 2004.

Svärd, M., Mattsson, K. and Nordström, J. Steady state computations using summation-by-parts operators. *Journal of Scientific Computing*, 24(1):79–95, September 2005.

Svärd, M. and Nordström, J. On the order of accuracy for difference approximations of initial-boundary value problems. *J. Comput. Physics*, 218(1):333–352, October 2006.